Supplementary Material

Activation of the HGF/c-Met axis in the tumor microenvironment: a multispecies model

Anna Konstorum[1] and John Lowengrub[2,3,4,5]

[1]Center for Quantitative Medicine, UConn Health, Farmington, CT, USA
[2]Department of Mathematics, University of California, Irvine, CA, USA
[3]Center for Complex Biological Systems, University of California, Irvine, CA, USA
[4]Department of Biomedical Engineering, University of California, Irvine, Irvine, CA, USA
[5]Chao Family Comprehensive Cancer Center, UC Irvine

S1 Nondimensionalization

The equations are nondimensionalized following (Wise et al., 2008; Youssefpour et al., 2012): we take the O diffusion length scale, $l = \sqrt{D_O/\nu_{UOSC}}$, and the mitosis time scale $\tau = (\lambda_{MSC_M}\bar{C}_{AO})^{-1}$, where here λ_{MSC_M} represents the midpoint of the minimum and maximum stem cell division rates. The diffusion length scale, l is estimated $l \sim 150\mu m$ and the mitosis time scale at $\tau \sim 1$ day following (Frieboes et al., 2006). The characteristic tumor pressure is taken to be $\bar{p} = l^2/(\tau\bar{\kappa})$, where $\bar{\kappa}$ is the characteristic value of the pressure-dependent cell-motility, κ. We also take $\bar{C}_{\mathrm{TGF}\beta}$ to be the characteristic concentration of TGFβ, $\bar{C}_M = (\nu_{PMI})^{-1}$, $\bar{C}_{MI} = \bar{C}_{AO}/(\nu_{PMI}\nu_{DM})$, $\bar{C}_{HGF} = \bar{C}_{AO}^2/(\bar{C}_{\mathrm{TGF}\beta})$, and $\bar{C}_{SGF} = \bar{C}_{AO}$. The conservation equations are then taken to be

$$\frac{\partial \phi_*'}{\partial t'} = -\nabla' \cdot \mathbf{J}_*' + Src_*' - \nabla' \cdot (\mathbf{u}_S \phi_*), \tag{S1}$$

where $*$ refers to tumor cell species (CSCs, TCs, or DCs). Nondimensionalized variables and parameters are presented in Tables S1 - S2, for brevity, c-Met is shortened to M and c-Met inhibitors to MI. For the nondimensionalized equations in the main text, all variables and parameters are presented without the prime notation.

Table S1: Nondimensional variables in Equations (1) - (14) and (23) - (31)

Tumor flux	$\mathbf{J}_*' = M_b' \phi_* \nabla \mu'$
Chemical Potential	$\mu' = (\partial F/\partial \phi_T)(\phi_T) - \varepsilon'^2 \nabla'^2 \phi_T$
Velocity	$\mathbf{u}_\mathbf{s}' = \mathbf{u}_\mathbf{s}/(l/\tau)$
Pressure	$p' = p/\bar{p}$
$[O]$	$C_O' = C_O/\bar{C}_{AO}$
[TGFβ]	$C_{TGF\beta}' = C_{TGF\beta}/\bar{C}_{TGF\beta}$
$[M]$	$C_M' = C_M/\bar{C}_M$
$[MI]$	$C_{MI}' = C_{MI}/\bar{C}_{MI}$
[HGF]	$C_{HGF}' = C_{HGF}/\bar{C}_{HGF}$
[SGF]	$C_{SGF}' = C_{SGF}/\bar{C}_{SGF}$

Table S2: Nondimensional parameters in Equations (1) - (14) and (23) - (31)

Mobility	$M_b' = \tau/\tau_M;\ \tau_M = l^2\varepsilon/(M_b \cdot \gamma)$	Pressure-dependent cell motility	$\kappa' = \kappa/\bar{\kappa}$
Diffuse interface thickness	$\varepsilon' = \varepsilon/l$	Global adhesion	$\gamma' = \tau/\tau_R;\ \tau_R = \gamma\bar{\kappa}/l^3$
Strength of M action on P_0	$\xi_0' = \xi_0 \cdot \bar{C}_M$	Strengh of TGFβ action on P_0	$\psi_0' = \psi_0 \cdot \bar{C}_{\mathrm{TGF}\beta}$
Strength of M action on λ_{MSC}	$\xi_1' = \xi_1 \cdot \bar{C}_M$	Strengh of TGFβ action on λ_{MSC}	$\psi_1' = \psi_1 \cdot \bar{C}_{\mathrm{TGF}\beta}$
TC mitosis rate	$\lambda_{MTC}' = \tau/\tau_{MTC};$ $\tau_{MTC} = (\lambda_{MTC}\bar{C}_{AO})^{-1}$	TC death rate	$\lambda_{ATC}' = \tau/\tau_{ATC};$ $\tau_{ATC} = (\lambda_{ATC})^{-1}$
DC lysis rate	$\lambda_L' = \tau \cdot \lambda_L$	Oxygen uptake rate	$\nu_{UOTC}' = \nu_{UOTC}/\nu_{UOSC}$
Oxygen transfer rate	$\nu_{PO}' = \nu_{PO}/\nu_{UOSC}$	TGFβ uptake rate by CSCs	$\nu_{\mathrm{UTGF}\beta}' = \tau_{\mathrm{TGF}\beta} \cdot \nu_{\mathrm{UTGF}\beta}$
TGFβ decay rate	$\nu_{\mathrm{DTGF}\beta}' = \tau_{\mathrm{TGF}\beta} \cdot \nu_{\mathrm{DTGF}\beta}$	TGFβ production rate by TCs	$\nu_{\mathrm{PTGF}\beta}' = \tau_{\mathrm{TGF}\beta} \cdot \nu_{\mathrm{PTGF}\beta};$ $\tau_{\mathrm{TGF}\beta} = l^2/D_{\mathrm{TGF}\beta}$
M diffusion rate	$D_M' = \tau/\tau_M;\ \tau_M = l^2/D_M$	MI diffusion rate	$D_{MI}' = \tau/\tau_{MI};\ \tau_{MI} = l^2/D_{MI}$
Strength of HGF-independent M activation	$\nu_0' = \nu_0$	Strength of HGF-induced M activation (1)	$\lambda_{1_{HGF}}' = \lambda_{1_{HGF}} \cdot \bar{C}_{HGF}$
Strength of HGF-induced M activation (2)	$\lambda_{2_{HGF}}' = \lambda_{2_{HGF}} \cdot \bar{C}_{HGF} \cdot \nu_{PMI}$	Ratio of λ_{MSC_M} to ν_{DM}	$R = \tau \cdot \nu_{DM}$
Background M production rate	$\mu_0' = \mu_0\bar{C}_{AO}/(\bar{C}_M\nu_{DM})$	MI decay rate	$\nu_{DMI}' = \nu_{DMI}/\nu_{DM}$
HGF production rate	$\nu_{PHGF}' = \tau \cdot \nu_{PHGF}$	Regularization constant	$\zeta' = \zeta/\bar{C}_{\mathrm{TGF}\beta}$
HGF decay rate	$\nu_{DHGF}' = \tau \cdot \nu_{DHGF}$	SGF production rate by SCs	$\nu_{SGFC}' = \tau \cdot \nu_{SGFC}$
SGF production rate by TCs	$\nu_{SGFT}' = \tau \cdot \nu_{SGFT}$	SGF decay rate	$\nu_{DSGF}' = \tau \cdot \nu_{DSGF}$
HGF diffusion rate	$D_{HGF}' = \tau/\tau_{HGF}; \tau_{HGF} = l^2/D_{HGF}$	SGF diffusion rate	$D_{SGF}' = \tau/\tau_{SGF}; \tau_{SGF} = l^2/D_{SGF}$

S2 Asymmetry in initialization and initial conditions for C_M, C_{MI}, C_{HGF}, and C_{SGF}

The initialized asymmetrical shape as seen in the inset in Figure 2(a) is created as follows

$$\phi_T(x,0) = \frac{1}{2}\left(1 - \tan h\left(\frac{I(x,y)-1}{2\sqrt{2}\varepsilon}\right)\right), \tag{S2}$$

$$I(x,y) = \frac{\sqrt{3} + r(x,y)}{\sqrt{x^2+y^2}+0.001}, \tag{S3}$$

where $r(x,y) = \sum_{i=1}^{2} a_i \cos(b_i\theta(x,y)) + \sum_{i=3}^{4} a_i \sin(b_i\theta(x,y))$, $\theta(x,y) = \tan^{-1}(y/x)$, $a_i \in (0,1)$, $b_i \in \mathbb{N}$ give the initial shape asymmetry. For specific values of $\{a_i, b_i\}$, we take $(a_1,a_2,a_3,a_4) = (0.2,0.1,0.1,0.1)$ and $(b_1,b_2,b_3,b_4) = (2,5,8,3)$. We then take $\phi_{CSC}(x,0) = 0.45 \cdot \phi_T(x,0)$, $\phi_{DC}(x,0) = 0.05 \cdot \phi_T(x,0)$, and $\phi_{TC}(x,0)$ can be solved for from the previous two equalities to obtain $\phi_{TC}(x,0) = 0.5 \cdot \phi_T(x,0)$.

The initial conditions for C_M and C_{MI}, the concentrations of M and MI, respectively, are taken to be $C_M(x,0) = (1.2 + 0.1(rand - 0.5))\phi_T$ and $C_{MI}(x,0) = 1.44\phi_T$, where *rand* is a random number uniformly distributed over $[0,1]$ and different at every point in the computational domain (the *rand* value used for each simulation remains the same for comparison purposes). The initial conditions for C_{HGF} and C_{SGF}, the concentrations of HGF and SGF, respectively, are taken to be $C_{HGF} = (1.0 + 0.1(rand - 0.5))\phi_H$ and $C_{SGF} = (1.0 + 0.1(rand - 0.5))\phi_T$.

S3 Cell-type specific SGF production

Simulations in the main text are based on the assumption that $\nu_{SGFS} = \nu_{SGFT}$, but this may not be the case. For example, stem (or terminal) cells may produce SGF at a much higher rate than the other tissue type, which may result in a different tumor growth phenotype. To investigate how the tumor would behave under different production rates of SGF by the two compartments, we simulate tumor growth under four different conditions: $\{\nu_{SGFS}, \nu_{SGFT}, \nu_{PHGF}\} = \{15,0,5\}, \{15,0,15\}, \{0,15,5\}, \{0,15,15\}$. The parameters ν_{SGFS}, ν_{SGFT}, and ν_{PHGF} are as described in Equations (23) and (24).

In Figure S1, we observe that production of SGF by only stem cells results in a phenotype qualitatively similar to the original results, whereas in the case of sole terminal cell production of SGF, we observe smaller stem cell spots that tend to cluster together and laterally self-renew along the tumor-host boundary when $\nu_{PHGF} = 15.0$. This is due to the higher probability of self-renewal near the stem cell spots and in the interior of the tumor due to the higher concentration of HGF along the tumor-host boundaries (Figure S1 (b)), causing stem cells to divide and self-renew laterally, rather than outward into the host tissue. Since the dynamics with only stem cell production of SGF are qualitatively similar to the stem and terminal cell SGF production, we maintain our assumption that $\nu_{\mathrm{SGFS}} = \nu_{\mathrm{SGFT}}$, as the resultant simulation behaves in a similar fashion to the most plausible biological scenarios (either $\nu_{SGFS} = \nu_{SGFT}$ or $\nu_{SGFS} >> \nu_{SGFT}$).

S4 Therapy

We consider how therapy acting on the HGF/c-Met axis can be modeled by changing two sets of parameters: $\lambda_{\{1,2\}_{HGF}}$, the strength of HGF effect on c-Met activation, and ν_0, the strength of c-Met auto-activation (see Equations (18) - (21)). Lowering $\lambda_{1,2_{HGF}}$ represents application of drugs that either inhibit HGF directly or block HGF binding and c-Met activation, while lowering ν_0 represents the class of drugs that inhibit c-Met auto-activation. Lowering both ν_0 along with $\lambda_{1,2_{HGF}}$ represents anti-c-Met therapy, either by kinase inhibition or inhibition of downstream pathway components (Figure S2). Two parameter alterations, termed T_1 and T_2, represent two therapies that are analyzed in the main text. A shorter T_2 therapy (from $T = 50$

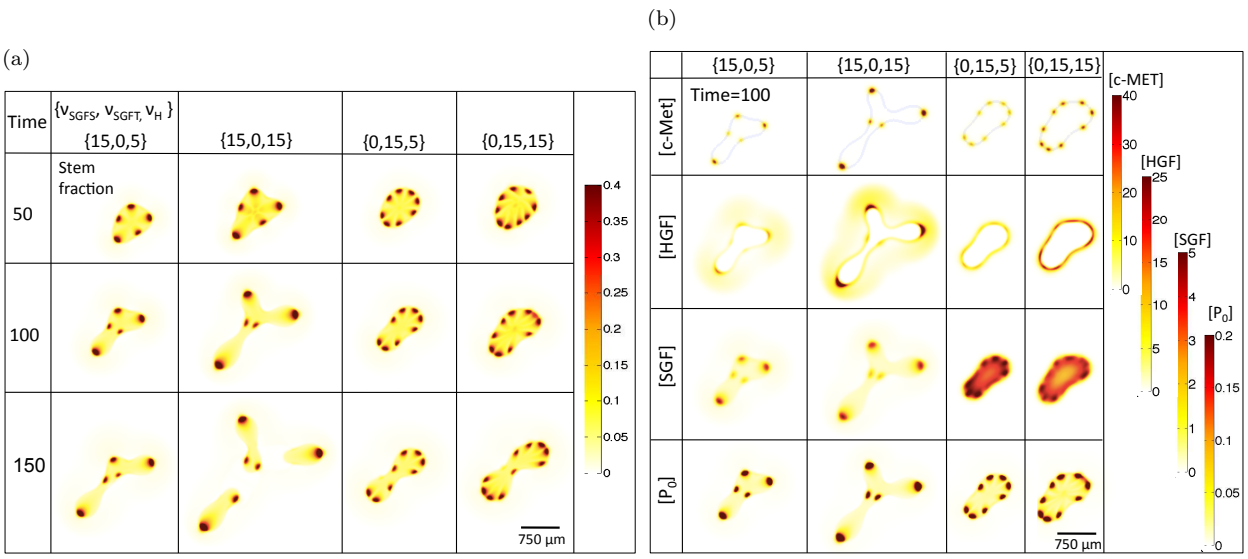

Figure S1: Cell-type specific SGF production
(a) Stem cell fraction for $T = 50, 100$, and 150 and (b) Chemical species and probability of self-renewal for $T = 100$. SGF production by tumor cells is not assumed to be identical for stem and tumor cells. The first two columns of (a) and (b) show simulation results from setting SGF production only by stem cells, whereas the last two columns show results from setting SGF production only by terminal cells. The strength of HGF response, ν_H, is also tested with $\nu_H = 5$ for the first and third columns and $\nu_H = 15$ for the second and fourth columns.

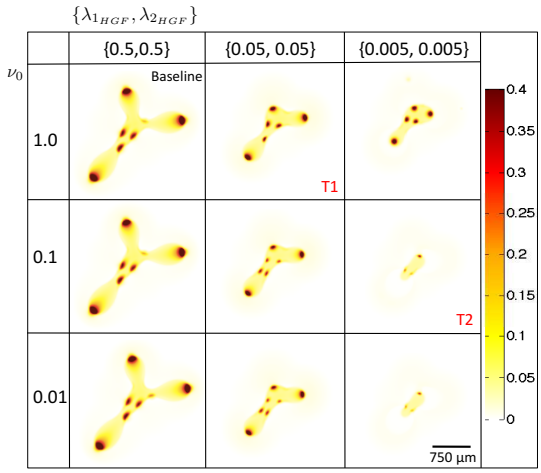

Figure S2: Stem cell fraction at $T = 100$ after therapy is applied at $T = 50$ to the high HGF condition. $\lambda_{1,2_{HGF}}$ is the strength of HGF effect on c-Met activation and ν_0 is the strength of autocrine c-Met activation.

to $T = 100$, and returning parameters to original conditions from $T = 100$ to $T = 150$) results in rapid tumor regrowth and fragmentation, indicating that long-term growth arrest would require surgical treatment and/or combination therapy (Figure S3).

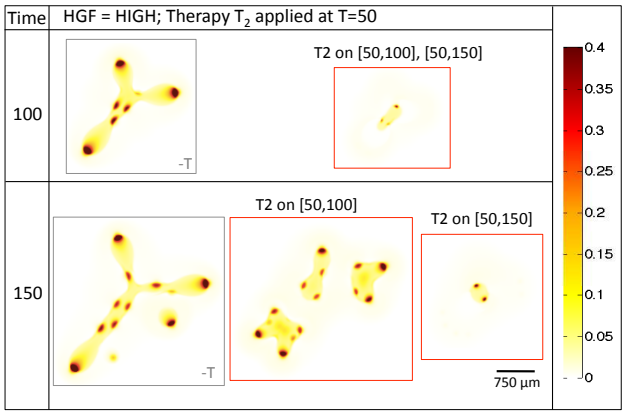

Figure S3: Stem cell fraction for high HGF condition at $T = 100$ and $T = 150$ with therapy T2 applied from $T = 50$ to $T = 100$ or to $T = 150$. Results in main text show therapy results from $T = 50$ to $T = 150$. Note that when therapy is only applied until $T = 100$, tumor regrowth occurs rapidly.

S5 References

References

Frieboes, H. B., Zheng, X., Sun, C.-H., Tromberg, B., Gatenby, R., Cristini, V., Feb 2006. An integrated computational/experimental model of tumor invasion. Cancer Res 66 (3), 1597–604.

Wise, S. M., Lowengrub, J. S., Frieboes, H. B., Cristini, V., Aug 2008. Three-dimensional multispecies nonlinear tumor growth–i model and numerical method. J Theor Biol 253 (3), 524–43.

Youssefpour, H., Li, X., Lander, A. D., Lowengrub, J. S., Jul 2012. Multispecies model of cell lineages and feedback control in solid tumors. J Theor Biol 304, 39–59.